Takafumi Yokota, Kenji Oritani, Karla P. Garrett, Taku Kouro, Makoto Nishida, Isao Takahashi, Michiko Ichii, Yusuke Satoh, Paul W. Kincade, **Yuzuru Kanakura**.	Soluble frizzled-related protein 1 is estrogen inducible in bone marrow stromal cells and suppresses the earliest events in lymphopoiesis.	J Immunol	181(9)	6061-6072	2008
Michiko Ichii, Kenji Oritani, Takafumi Yokota, Makoto Nishida, Isao Takahashi, Takahiro Shirogane, **Sachiko Ezoe**, Saitoh N, Rie Tanigawa, Paul W. Kincade, **Yuzuru Kanakura**.	Regulation of human B lymphopoiesis by the transforming growth factor-beta superfamily in a newly established coculture system using human mesenchymal stem cells as a supportive microenvironment.	Exp Hematol	36(5)	587-957	2008
Yamauchi A, Ikeda J, Nakamichi I, Kohara M, Fukuhara S, Hino M, **Kanakura Y**, Ogawa H, Sugiyama H, Kanamaru A, Aozasa K; Osaka Lymphoma Study Group.	Diffuse large B-cell lymphoma showing an interfollicular pattern of proliferation: a study of the Osaka Lymphoma Study Group.	Histopatholog y	52	731-737	2008
Nojima J, Masuda Y, Iwatani Y, Kuratsune H, Watanabe Y, Suehisa E, Takano T, Hidaka Y, **Kanakura Y**.	Arteriosclerosis obliterans associated with anti-cardiolipin antibody/beta2-glycoprotein I antibodies as a strong risk factor for ischaemic heart disease in patients with systemic lupus erythematosus.	Rheumatology (Oxford)	47(5)	684-689	2008
H Murota, S Bae, Y Hamasaki, R Maruyama, **I Katayama**.	Emedastine difumarate inhibits histamine-induced collagen synthesis in dermal fibroblasts.	J Investig Allergol Clin Immunol	18(4)	245-252	2008
Hiroyuki Murota, Yorihisa Kotobuki, Noriko Umegaki, Mamori Tani, **Ichiro Katayama**	New aspect of anti-inflammatory action of lipo-prostaglandinE1 in the management of collagen diseases-related skin ulcer.	Rheumatol Int	28(11)	1127-1135	2008
Akiko Kijima, Shigeki Inui, Toshiaki Nakamura, Satoshi Itami and **Ichiro Katayama**	Does drug-induced hypersensitivity syndrome elicit bullous pemphigoid?	Allergol Int	57(2)	181-182	2008

Takaaki Hanafusa, Yuji Yamaguchi, Motoki Nakamura, Mamori Tani, Akimichi Morita, **Ichiro Katayama**	Establishment of suction blister roof grafting by injection of local anesthesia beneath the epidermis: less painful and more rapid formation of blisters.	J Dermatol Sci	50(3)	243-247	2008
Zhu P, Hata R, Cao F, Gu F, Hanakawa Y, **Hashimoto K**, Sakanaka M	Ramified microglial cells promote astrogliogenesis and maintenance of neural stem cells through activation of Stat3 function.	FASEB J.	22	3866-77	2008
Tohyama M, Shirakata Y, Sayama K, **Hashimoto K**	A marked increase in serum soluble Fas ligand in drug-induced hypersensitivity syndrome.	Br J Dermatol.	159	981-4	2008
Nanba D, Inoue H, Shigemi Y, Shirakata Y, **Hashimoto K**, Higashiyama S	An intermediary role of proHB-EGF shedding in growth factor-induced c-Myc gene expression.	J Cell Physiol	214	465-73	2008
Isokame M, Hieda M, Hirakawa S, Shudou M, Nakashiro K, **Hashimoto K**, Hamakawa H, Higashiyama S	Plasma-membrane-anchored growth factor pro-amphiregulin binds A-type lamin and regulates global transcription.	J Cell Sci	121	3608-18	2008
Dai X, Sayama K, Shirakata Y, Tokumaru S, Yang L, Tohyama M, Hirakawa S, Hanakawa Y, **Hashimoto K**	PPARgamma is an important transcription factor in 1alpha,25-dihydroxyvitamin D3-induced involucrin expression.	J Dermatol Sci	50	53-60	2008
Dai X, Sayama K, Tohyama M, Shirakata Y, Yang L, Hirakawa S, Tokumaru S, **Hashimoto K**	The NF-kB, p38 MAPK and STAT1 pathways differentially regulate the dsRNA-mediated innate immune responses of epidermal keratinocytes.	Int Immunol.	20	901-9	2008
Watanabe H, Daibata M, Tohyama M, Batchelor J, **Hashimoto K**, Iijima M	Chromosomal integration of human herpesvirus 6 DNA in anticonvulsant hypersensitivity syndrome.	Br J Dermatol	158	640-642	2008

STEM CELLS
TISSUE-SPECIFIC STEM CELLS

Circulating Bone Marrow-Derived Osteoblast Progenitor Cells Are Recruited to the Bone-Forming Site by the CXCR4/Stromal Cell-Derived Factor-1 Pathway

SATORU OTSURU,[a,b] KATSUTO TAMAI,[a] TAKEHIKO YAMAZAKI,[a] HIDEKI YOSHIKAWA,[b] YASUFUMI KANEDA[a]

[a]Division of Gene Therapy Science and [b]Department of Orthopaedic Surgery, Osaka University Graduate School of Medicine, Osaka, Japan

Key Words. Bone marrow cells • Chemokine receptor CXCR4 • Mobilization kinetics • Osteoblast • Peripheral blood Stromal derived factor-1 • Stem/progenitor cell • Tissue regeneration

ABSTRACT

Previous studies demonstrated the existence of osteoblastic cells in circulating blood. Recently, we reported that osteoblast progenitor cells (OPCs) in circulation originated from bone marrow and contributed to the formation of ectopic bone induced by implantation of a bone morphogenetic protein (BMP)-2-containing collagen pellet in mouse muscular tissue. However, the character of circulating bone marrow-derived osteoblast progenitor cells (MOPCs) and the precise mechanisms involving the circulating MOPCs in the osteogenic processes, such as signals that recruit the circulating MOPCs to the osseous tissues, have been obscure. In this report, we demonstrated for the first time that the MOPCs were mobilized from intact bones to transiently occupy approximately 80% of the mononuclear cell population in the circulating blood by BMP-2-pellet implantation. The mobilized MOPCs in the circulation did not express the hematopoietic marker CD45 on their surface, but they expressed CD44 and CXCR4, receptors of osteopontin and stromal cell-derived factor-1 (SDF-1), respectively. The MOPCs isolated from the mouse peripheral blood showed the ability to be osteoblasts in vitro and in vivo. Furthermore, the MOPCs in the circulation efficiently migrated to the region of bone formation by chemoattraction of SDF-1 expressed in vascular endothelial cells and the de novo osteoblasts of the region. These data may provide a novel insight into the mechanism of bone formation involving MOPCs in circulating blood, as well as perspective on the use of circulating MOPCs to accelerate bone regeneration in the future.
STEM CELLS *2008;26:223–234*

Disclosure of potential conflicts of interest is found at the end of this article.

INTRODUCTION

Bone marrow contains hematopoietic stem cells and mesenchymal stem/progenitor cells (MPCs) that can differentiate into various mesenchymal tissues, such as bone, cartilage, fat, and muscle [1–3]. These cells are also found in various mesenchymal tissues [4], although the relationship between the marrow mesenchymal stem/progenitor cells (MMPCs) and extramarrow MPCs has not been fully understood. Marrow MPCs have been shown to engraft not only in bone marrow but also in multiple mesenchymal tissues after systemic infusion [3, 5], suggesting that circulating blood might be a natural route for MMPC migration to the mesenchymal tissues in vivo.

Previous studies have shown the existence of osteoblast-lineage cells in the circulating blood of various mammals, including humans [6–8]. The circulating osteoblast-lineage cells were shown to form bone in culture and in transplanted animals [6]. Studies have also reported more circulating osteoblast-lineage cells during the adolescent growth spurt than in adulthood [6]. However, the origin and the functional role of those osteoblastic cells in human circulation are unclear.

Bone morphogenetic protein (BMP)-2 and other members of the BMP family are well-known inducers of bone formation in vitro and in vivo [9]. In the process of a fracture healing, BMP stimulation recruits MPCs to the fracture lesion and induces their differentiation into osteoblasts. An experimental model has also indicated that BMP-2 stimulation is essential for ectopic bone formation when BMP-2 is transplanted in the back muscles of mice [10]. Recently, we reported that marrow-derived osteoblast progenitor cells (MOPCs) in circulating blood participated in BMP-2-induced ectopic bone formation [11]. If circulating MOPCs play a major role in bone regeneration in vivo, efficient recruitment of MOPCs from bone marrow to the lesion seems to be critical to obtain mature and sufficient regeneration. However, the character of circulating MOPCs and precise mechanisms involving the MOPCs in the osteogenic processes, such as signals that recruit circulating MOPCs to the osseous tissues, have been obscure.

In this study, we characterized MOPCs in the circulating blood without expansion in culture and showed that MOPCs were mobilized in the circulation after stimulation with tissue injury, migrated to damaged tissues by chemoattraction of stromal cell-derived factor-1 (SDF-1), and provided a significant number of mature osteoblasts with BMP-2 stimulation during bone formation. We believe these findings provide novel insights into bone regeneration involving circulating MOPCs.

Correspondence: Katsuto Tamai, M.D., Ph.D., Division of Gene Therapy Science, Osaka University Graduate School of Medicine, 2-2 Yamada-oka, Suita, Osaka 565-0871, Japan. Telephone: 81-6-6879-3901; Fax: 81-6-6879-3909; e-mail: tamai@gts.med.osaka-u.ac.jp Received July 1, 2007; accepted for publication September 28, 2007; first published online in STEM CELLS *EXPRESS* October 11, 2007. ©AlphaMed Press 1066-5099/2007/$30.00/0 doi: 10.1634/stemcells.2007-0515

MATERIALS AND METHODS

Bone Marrow Transplantation

Under sterile conditions, bone marrow cells were isolated from 8- to 10-week-old male C57BL/6 transgenic mice that ubiquitously expressed enhanced green fluorescent protein (GFP) [12]. Eight- to 10-week-old female C57BL/6 mice were lethally irradiated with 10 Gy. For total bone marrow transplantation (BMT), each irradiated recipient received 5×10^6 bone marrow cells from GFP transgenic mice. For CD45/GFP double-positive BMT, the CD45-positive bone marrow cells of GFP transgenic mice were sorted using the magnetic cell sorting (MACS) system (Miltenyi Biotec, Bergisch Gladbach, Germany, http://www.miltenyibiotec.com). Each irradiated recipient received 4.5×10^6 CD45-positive marrow cells of GFP transgenic mice in combination with 0.5×10^6 CD45-negative marrow cells of wild-type mice. All BMT mice were used at least 6 weeks after BMT. All animals were handled according to approved protocols and the guidelines of the Animal Committee of Osaka University.

Parabiotic Mouse Model

The parabiotic mouse model was generated as previously described [13]. A total BMT mouse and a wild-type mouse (C57/BL6) were sutured from the olecranon to the knee joint on the corresponding lateral aspects.

Preparation and Implantation of BMP-2-Containing Collagen Pellets

Recombinant human BMP-2 was provided by Astellas Pharma Inc. (Tokyo, http://www.astellas.com). The BMP-2 was suspended in buffer solution (5 mmol/l glutamic acid, 2.5% glycine, 0.5% sucrose, and 0.01% Tween 80, pH 4.5) at a concentration of 1 μg/μl. Next, 3 μl (3 μg of BMP-2) of the BMP-2 solution was diluted in 22 μl of phosphate-buffered saline (PBS) and blotted into a porous collagen disc (6 mm diameter, 1 mm thickness), freeze-dried, and stored at −20°C. All procedures were carried out under sterile conditions. BMP-2-containing or control PBS-containing collagen pellets were implanted on the backs of BMT mice, parabiotic mice, C57BL/6 mice, or nude mice. Three weeks later, fluorescent photos of ectopic bones were taken using a digital microscope (Multiviewer system VB-S20; Keyence, Osaka, Japan, http://www.keyence.com).

Immunohistochemistry and Analysis

The ectopic bones were removed and fixed with 4% paraformaldehyde at 4°C for 48 hours. After soft x-ray photos were taken, bones were decalcified with EDTA solution at 4°C for 6 days. The EDTA solution was changed every other day. After decalcification, the pellets were equilibrated in PBS containing 15% sucrose for 12 hours and then in PBS containing 30% sucrose for 12 hours, embedded in Tissue-Tek OCT Compound (Sakura Finetek, Tokyo, http://www.sakuraeu.com), frozen on dry ice, and stored at −20°C.

For immunofluorescence staining, 6-μm-thick sections were cut with a cryostat (Leica Microsystems AG, Wetzlar, Germany, http://www.leica.com). After washing, the sections were treated with 0.1% trypsin (Difco Laboratories, Detroit, MI, http://www.bd.com/ds) in PBS for 30 minutes at 37°C to activate antigens. Then, those sections were blocked with normal goat serum for 1 hour before incubation with polyclonal anti-mouse osteocalcin antibody (1:250; Takara Bio, Shiga, Japan, http://www.takara-bio.com) or polyclonal anti-mouse SDF-1a antibody (1:250; eBioscience Inc., San Diego, http://www.ebioscience.com). Subsequently, sections were stained with Alexa Fluor 546 goat anti-rabbit IgG secondary antibody (Molecular Probes, Eugene, OR, http://probes.invitrogen.com) for 2 hours. Then, sections were stained with 4′,6-diamidino-2-phenylindole (DAPI) for 10 minutes at room temperature and mounted with the antifade solution Vectashield (Vector Laboratories, Burlingame, CA, http://www.vectorlabs.com).

For staining endothelial progenitor cells and tissues around the pellets, the pellets were removed daily until day 7 after implantation. After removal, pellets were embedded in Tissue-Tek OCT Compound and frozen on dry ice. Six-micrometer-thick sections were blocked with normal goat serum for 1 hour before incubation with monoclonal anti-mouse CD31 antibody (1:250; BD Pharmingen, San Jose, CA, http://www.bdbiosciences.com/index_us.shtml), monoclonal anti-mouse CD34 antibody (1:100; BD Pharmingen), monoclonal anti-smooth-muscle actin antibody (1:250; Sigma-Aldrich, St. Louis, http://www.sigmaaldrich.com), or polyclonal anti-mouse SDF-1a antibody (1:250; eBioscience). Subsequently, sections were stained with Alexa Fluor 546 goat anti-rat IgG secondary antibody, Alexa Fluor 488 anti-rat IgG secondary antibody, or Alexa Fluor 488 anti-mouse IgG secondary antibody (Molecular Probes) with M.O.M. Kit (Vector Laboratories) for 2 hours. The sections were mounted with antifade solution Vectashield after 10 minutes of DAPI staining. All pictures were taken with a confocal laser microscope, model Radiance 2100 using LaserSharp 2000 software (Bio-Rad Japan, Tokyo, http://www.bio-rad.com). To assess the frequency of MOPCs for osteoblast differentiation, we counted the number of GFP-positive cells in the osteocalcin-positive osteoblasts lining the trabecular bone. The ratio was quantitatively calculated in at least five low-power visual fields.

Peripheral Blood Mononuclear Cell Isolation

Peripheral blood was taken from the heart with a 24-gauge needle and 1-ml syringe containing heparin and enriched for low-density mononuclear cells by Ficoll-Paque (Amersham Biosciences, Uppsala, Sweden, http://www.amersham.com) centrifugation. Red blood cells were removed by resuspending in 0.125% Tris-NH_4Cl buffer and sieving through a nylon mesh. Isolated peripheral blood mononuclear cells (PBMNCs) from BMP-2 pellet-implanted mice were reacted with anti-mouse CD45 microbeads (Miltenyi Biotec), and the CD45-negative cells dominantly containing MOPCs were sorted using the MidiMACS system (Miltenyi Biotec) according to the manufacturer's protocol.

In Vitro Differentiation

For induction of osteoblast differentiation in culture, MACS-sorted CD45-negative PBMNCs from BMP-2-implanted GFP transgenic mice were plated on a 24-well plate. The sorted cells were then inoculated in basal medium consisting of Dulbecco's modified Eagle's medium (DMEM) supplemented with 10% fetal calf serum (FCS), 100 U/ml streptomycin/penicillin, and 50% conditioned culture medium (DMEM with 10% FCS) of mouse bone marrow mesenchymal cells as a growth factor supplement (S. Otsuru and K. Tamai, unpublished data). To induce osteoblast differentiation, 300 ng/ml BMP-2 was added to the culture medium for 3 weeks. In some experiments, the sorted CD45-negative PBMNCs were cultured in the osteogenic medium consisting of Iscove's modified Dulbecco's medium supplemented with 0.1 μM dexamethasone (Nacalai Tesque Inc., Kyoto, Japan, http://www.nacalai.co.jp/en), 10 mM β-glycerol phosphate (Sigma-Aldrich), and 0.05 mM ascorbic acid 2-phosphate (Sigma-Aldrich) for 3–4 weeks.

Alizarin Red S Staining

To observe calcium deposition, cells were fixed with 4% paraformaldehyde and stained with 2% alizarin red S (Nacalai Tesque) solution in water for 10 minutes. Excess stain was removed by several washes with distilled water.

Alkaline Phosphatase Assay

Alkaline phosphatase (ALP) activity was assessed as previously described [14]. Cell lysates were centrifuged, and supernatants were used for the enzyme assay. Alkaline phosphatase activity was measured according to the methods of Kind-King, using a test kit (Wako Chemical, Osaka, Japan, http://www.wako-chem.co.jp/english)

with phenylphosphate as a substrate. Enzyme activity was expressed in King-Armstrong units, normalized to protein concentration.

In Vivo Bone Forming Assay

Fully open interconnected porous calcium hydroxyapatite ceramics were synthesized by adopting a "foam-gel" technique from a slurry of hydroxyapatite (60% wt/wt) with a cross-linking substrate (polyethyleneimine, 40% wt/wt) as previously reported [15]. Blocks of the ceramics were cut and shaped into 5-mm-diameter disks that were 2 mm thick. Cell culturing in the pores of the ceramics was performed as previously reported [16, 17]. The ceramic disk was soaked in 200 μl of CD45-negative cultured PBMNC suspension from GFP-transgenic mice in normal medium (10^6 cells per milliliter). After overnight incubation in a 96-well plate, normal medium was changed to osteogenic medium. The medium was renewed three times a week, and the cultures were maintained for 2 weeks. After a wash with PBS, the disks were implanted under the muscular fascia in the backs of nude mice. Disks without cells were also implanted as controls. Eight weeks later, the disks were harvested and fixed in 4% paraformaldehyde. After decalcification with K-CX (Falma Co., Osaka, Japan; http://www.falma.co.jp), the disks were embedded in paraffin, and the sections were stained with hematoxylin and eosin.

For immunofluorescence staining, the sections were treated with 0.1% trypsin (Difco Laboratories) in PBS for 30 minutes at 37°C to activate antigens. Next, those sections were blocked with normal goat serum for 1 hour before incubation with polyclonal anti-GFP antibody (1:250; MBL International Corp., Nagoya, Japan, http://www.mblintl.com). Subsequently, sections were stained with Alexa Fluor 488 goat anti-rabbit IgG secondary antibody (Molecular Probes) for 2 hours. Sections were then stained with DAPI for 10 minutes at room temperature and mounted with the antifade solution Vectashield (Vector Laboratories).

RNA Extraction and Reverse Transcription-Polymerase Chain Reaction

Total RNA was prepared with an RNeasy Kit (Qiagen, Tokyo, http://www1.qiagen.com) according to the manufacturer's protocol. Reverse transcription was performed by conventional protocols with Superscript reverse transcriptase (Invitrogen, Carlsbad, CA, http://www.invitrogen.com), and polymerase chain reaction (PCR) amplification was performed using the following primer sets: Cbfa1 (NM_009820, 289 base pairs [bp]), 5′-CCGCACGACAACCGCACCAT-3′ (forward) and 5′-CGCTCCGGCCCACAAATCTC-3′ (reverse); osteopontin (NM_009263, 437 bp), 5′-TCACCATTCGGATGAGTCTG-3′ (forward) and 5′-ACTTGTGGCTCTGATGTTCC-3′ (reverse); ALP (NM_007431, 180 bp), 5′-CGCCAGAGTACGCTCCCGCC-3′ (forward) and 5′-TGTACCCTGAGATTCGT-3′ (reverse); osteocalcin (X04142, 350 bp), 5′-CTGACCTCACAGATCCCAAG-3′ (forward) and 5′-GGAGCTGCTGTGACATCC-3′ (reverse); and SDF-1 (NM_021704, 538 bp), 5′-ACGCCAAGGTGGTCGCCGTGCTGG-3′ (forward) and 5′-GTTAGGGTAATACAATTCCTTAGA-3′ (reverse).

Flow Cytometry

Isolated PBMNCs were suspended in 100 μl of PBS containing fluorescein isothiocyanate (FITC)-conjugated anti-mouse CD45; phycoerythrin (PE)-conjugated anti-mouse CD11b, CD31, CD34, CD44, Flk-1, and Sca-1 (BD Pharmingen); and biotin-conjugated anti-mouse Gr-1 and CXCR4 (BD Pharmingen). Cells were then incubated for 30 minutes at 4°C in the dark. Subsequently, cells were stained with Streptavidin PE or Streptavidin PerCP (BD Pharmingen) or anti-rat IgG secondary antibody or anti-goat IgG secondary antibody (Molecular Probes) for 30 minutes at 4°C in the dark.

For the time-course analysis of the CD45-negative population in PBMNCs, BMP-2 pellets were implanted on the backs of 8- to 10-week-old female C57BL/6 mice daily, one mouse per day, for 7 days. At day 7, blood samples were taken, and hemolyzed PBMNCs were harvested. The harvested PBMNCs were reacted with FITC-conjugated anti-mouse CD45. Flow cytometry analysis was performed with a FACScan instrument using CellQuest software (Becton, Dickinson and Company, San Diego, http://www.bd.com).

In Vitro Migration Assay

After different concentrations of SDF-1a (R&D Systems Inc., Minneapolis, http://www.rndsystems.com) were added to the lower chamber, the 5×10^5 isolated CD45-negative PBMNCs from BMP-2 pellet-implanted mice in 100 μl of DMEM without growth factors were applied to the upper chamber of the membrane of the 96-well cell migration kit (Chemicon, Temecula, CA, http://www.chemicon.com). Some cells were pretreated with a CXCR4-blocking antibody (2B11; BD Pharmingen). After 4 hours of incubation at 37°C, the migratory cells on the bottom of the insert membrane were dissociated from the membrane by incubation with cell detachment buffer. These cells were stained with CyQuant GR dye (Molecular Probes, Eugene, OR, http://probes.invitrogen.com), and the fluorescence was measured with a fluorescence plate reader.

In Vivo Migration Assay

For the transplantation experiment, nude mice implanted with BMP-2-containing collagen pellets were injected via a tail vein with sorted CD45-negative PBMNCs with or without CXCR4-blocking antibody (2B11; BD Pharmingen) pretreatment from the GFP-transgenic BMP-2-implanted mice for 7 days.

Real-Time PCR

Primers and probes for hypoxia inducible factor-1 (HIF-1), SDF-1, and glyceraldehyde-3-phosphate dehydrogenase were purchased from Applied Biosystems (Foster City, CA, http://www.appliedbiosystems.com). Real-time PCR was carried out and measured by the ABI Prism 7900HT Sequence Detection System using SDS 2.2 software (Applied Biosystems).

Statistical Analysis

All experiments were repeated four to seven times. Statistical analyses were performed with the unpaired t test or the paired Student t test. p values <0.05 were considered statistically significant.

RESULTS

Bone Marrow-Derived Osteoblast Progenitor Cells in Circulation Contribute to BMP-2-Induced Ectopic Bone Formation

We have already reported that osteoblast progenitor cells (OPCs) were recruited from bone marrow to the circulating blood and contributed to the BMP-2-induced ectopic bone formation [11]. To obtain more direct evidence that circulating MOPCs were recruited to the region of the BMP-2 pellet to generate ectopic bone, we established a mouse model with parabiotic pairings that shared a circulatory system between a wild-type mouse and a GFP-BMT mouse (Fig. 1A) [13]. In our parabiotic mouse model, a wild-type mouse was surgically connected with a GFP-BMT mouse whose bone marrow had been replaced by GFP-transgenic bone marrow cells. The wild-type mouse can receive bone marrow-derived GFP-positive circulating cells from the GFP-BMT mouse after they develop shared circulation in a few weeks. We implanted a BMP-2 pellet into the wild-type mouse of the parabiotic pairings (Fig. 1A). Three weeks after transplantation, GFP fluorescence was detected at the region where the ectopic bone had formed (Fig. 1B). Histologic analysis revealed that 24.5% ± 3.1% of the osteoblasts that aligned on the regenerating bone and expressed osteocalcin (OC) were GFP-positive cells that originated from the bone marrow of the GFP-BMT mouse (Fig. 1C; supplemental online Fig. 1).

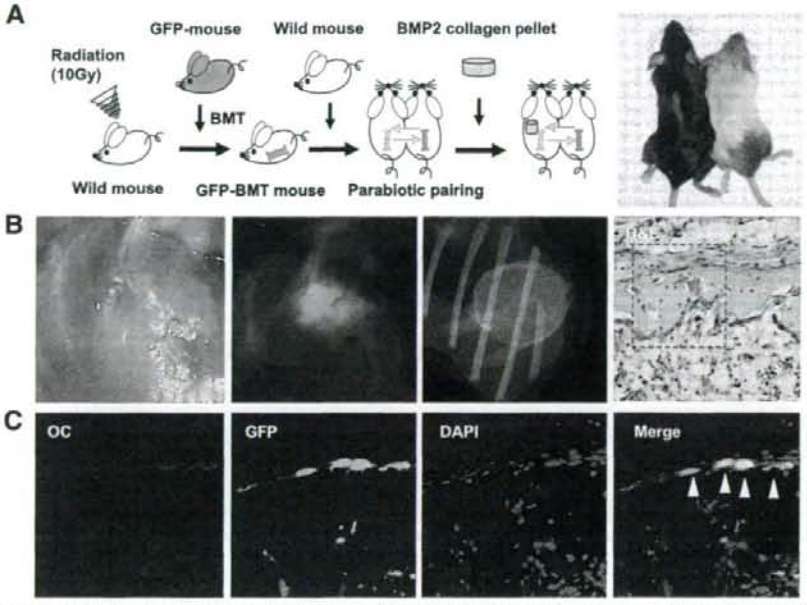

Figure 1. Bone marrow-derived osteoblast progenitor cells contribute to BMP-2-induced ectopic bone formation via circulation in a parabiotic mouse. **(A):** Parabiotic pairing between a GFP-BMT mouse and a wild-type mouse. A BMP-2 pellet was implanted into the wild-type mouse that could receive GFP-positive bone marrow cells from the GFP-BMT mouse through the circulation. **(B):** A BMP-2 pellet showed accumulation of GFP fluorescence 3 weeks after implantation under the muscular fascia of a wild-type parabiotic mouse. A soft x-ray photo of the BMP-2 pellet 3 weeks after the implantation demonstrated that ectopic bone formed in the BMP-2 pellet. Histologic section stained with H&E of the BMP-2 pellet 3 weeks after implantation also revealed bone formation in the BMP-2 pellet. Magnification, ×200. **(C):** Immunofluorescence staining of the boxed region in the H&E section showed that the cells lining the newly generated bone were osteoblasts expressing OC. Some of those osteoblasts expressing osteocalcin also exhibited GFP fluorescence (arrowheads). Magnification, ×600. Abbreviations: BMP, bone morphogenetic protein; BMT, bone marrow transplantation; DAPI, 4',6-diamidino-2-phenylindole; GFP, green fluorescent protein; OC, osteocalcin.

If both mice provide the bone marrow cells equally, these data suggest that approximately 50% of the regenerating osteoblasts may be derived from endogenous circulating MOPCs in parabiotic mice.

CD45-Negative Fraction in Bone Marrow Is a Major Source of Circulating MOPCs

We next examined a particular population in bone marrow to determine the major source of the circulating MOPCs. To determine whether the major source of MOPCs in bone marrow is CD45-positive or CD45-negative, we transplanted two types of bone marrow cells in combination to a lethally irradiated mouse before BMP-2-pellet implantation: a combination of CD45-negative/GFP-negative bone marrow cells and CD45-positive/GFP-positive bone marrow cells to generate CD45/GFP-BMT (Fig. 2A). The ectopic bone formed in the CD45/GFP-BMT mouse showed less accumulation of GFP fluorescence than that in the GFP-BMT mouse (Fig. 2B, 2C). Histologic examination revealed that the transplanted cells with a reduced CD45-negative/GFP-positive fraction formed ectopic bone with significantly fewer GFP-positive osteoblasts (11.0% ± 3.4%) than the controls (43.4% ± 10.6%, $p = .00127$; Fig. 2D). These data suggested that CD45-negative cells in bone marrow might be the major source of circulating MOPCs in BMP-2-implanted mice, although the contribution of CD45-positive cells to ectopic bone formation can not be completely excluded.

Kinetic Analysis of Circulating MOPCs

The data obtained led us to further characterize the kinetics of CD45-negative cell migration from bone marrow to circulating blood. To view CD45-negative cells in the circulation, five sets of the experiment were performed independently. In each experiment, seven mice were serially implanted (i.e., one mouse per day) with a BMP-2 pellet, and at day 7, they were all at once subjected to flow cytometry analysis to evaluate the CD45-negative cell populations in the PBMNCs. Before the implantation, the basal population of the CD45-negative cells in PBMNCs was less than 20%, possibly containing a remnant fraction of red blood cells even after the conventional PBMNC isolation procedure. Surprisingly, large increases of the CD45-negative population in PBMNCs, up to 83% frequency, were observed within 7 days after BMP-2-pellet implantation, coinciding with a significant reduction in the CD45-negative population in bone marrow cells within 7 days after BMP-2 implantation (Fig. 3A). A similar increase in the CD45-negative population in PBMNCs was observed at least once within 7 days after BMP-2-implantation in the other four sets of experiments. The induction of CD45-negative population in PBMNCs at the peak in each set of experiments was significantly higher in the BMP-2-implanted mice than in the control mice ($p = .0000142$; Fig. 3B). Implantation of empty collagen pellets also showed a relatively smaller but significant induction of the CD45-negative population in PBMNCs at the peak ($p = .0198$; Fig. 3B).

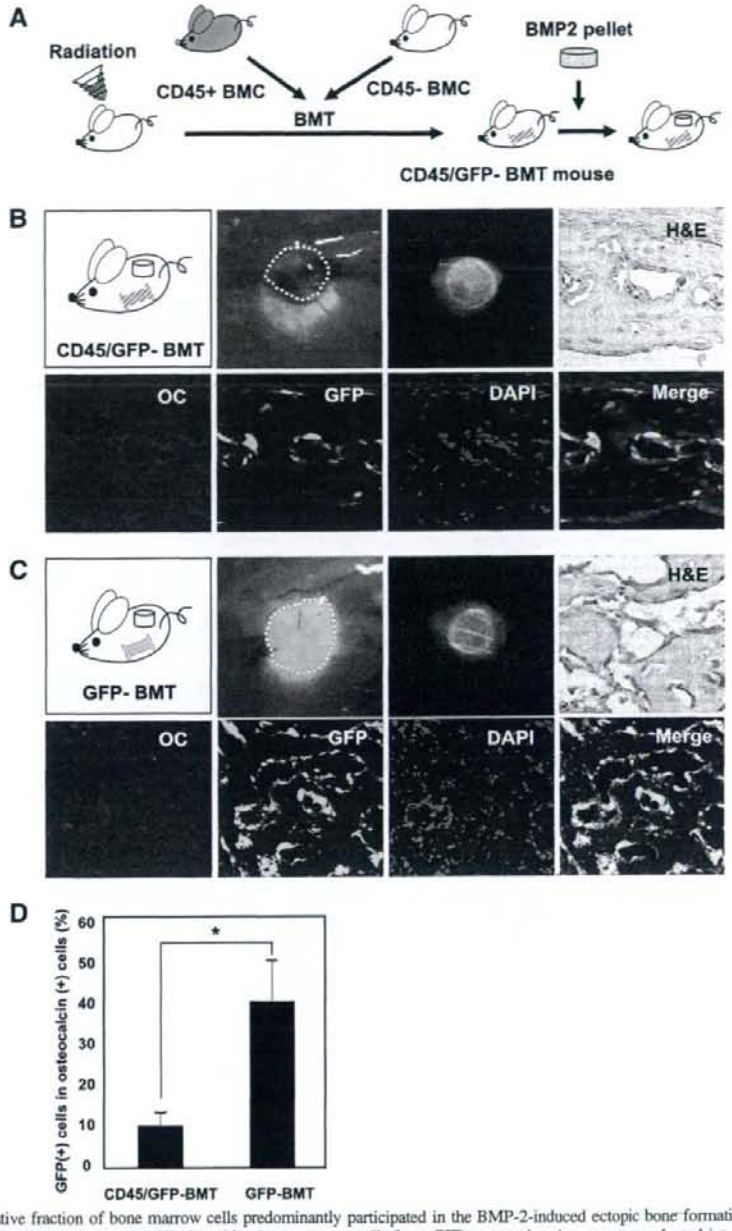

Figure 2. CD45-negative fraction of bone marrow cells predominantly participated in the BMP-2-induced ectopic bone formation. **(A):** CD45-negative bone marrow cells from wild-type mice and CD45-positive bone marrow cells from GFP-transgenic mice were transplanted into a lethal-dose-irradiated wild-type mouse (CD45/GFP-BMT) before the BMP-2-pellet implantation. **(B):** The ectopic bone (circled with a dotted line) in the CD45/GFP-BMT mouse showed weak GFP fluorescence. A soft x-ray photo and H&E-stained histologic section showed successful ectopic bone formation in the CD45/GFP-BMT mice. Immunofluorescence staining revealed fewer GFP-positive cells in the ectopic bone of the CD45/GFP-BMT mice than in the ectopic bone of the GFP-BMT mice. Magnification, ×400. **(C):** Total bone marrow cells from GFP transgenic mice were transplanted to lethally irradiated wild-type mice (GFP-BMT mouse). A BMP-2 pellet in the GFP-BMT mouse showed stronger GFP fluorescence (circled with a dotted line). A soft x-ray photo and histologic H&E-stained section showed bone formation in the BMP-2 pellet in the GFP-BMT mice as well. Immunofluorescence staining revealed that more GFP-positive cells expressed OC in the newly formed bone. Magnification, ×200. **(D):** Quantitative analysis showed that the percentage of GFP-positive/osteocalcin-positive osteoblasts in the osteocalcin-positive osteoblasts lining the trabecular bone significantly decreased in the CD45/GFP-BMT mice compared with the GFP-BMT mice. *, $p = .00127$. Abbreviations: BMC, bone marrow cell; BMP, bone morphogenetic protein; BMT, bone marrow transplantation; DAPI, 4′,6-diamidino-2-phenylindole; GFP, green fluorescent protein; OC, osteocalcin.

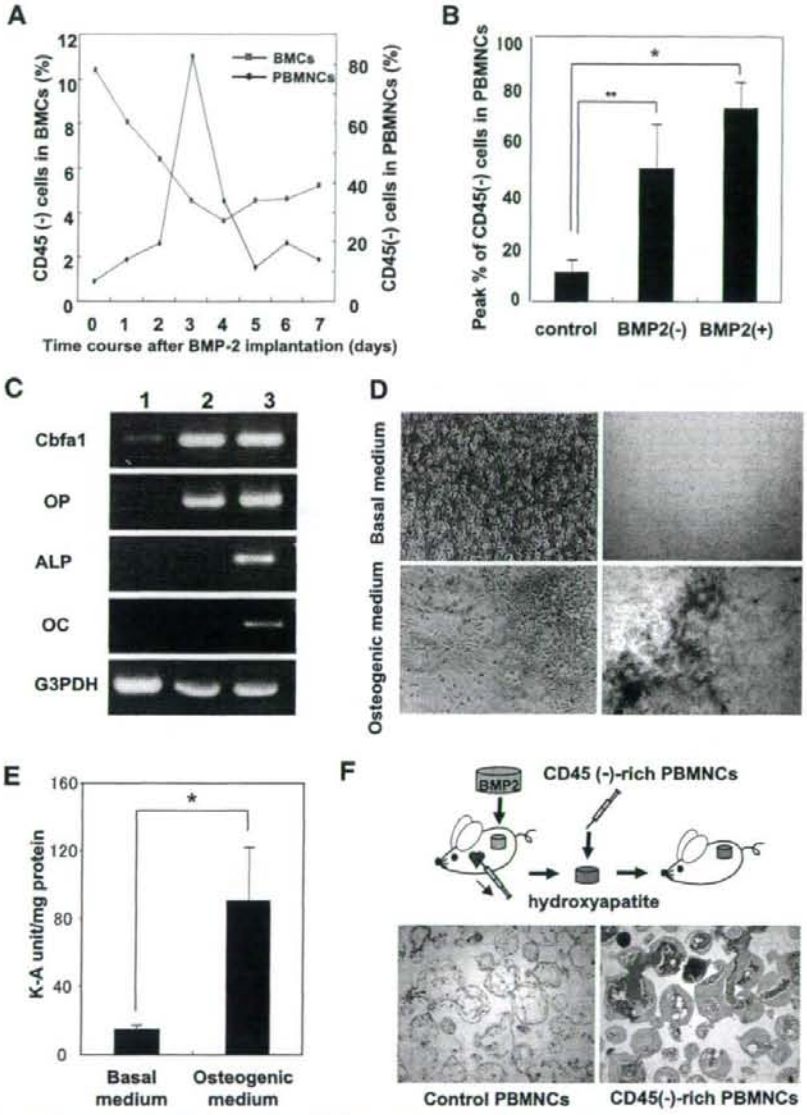

Figure 3. MOPCs were detected in PBMNCs from BMP-2 pellet-implanted mice. **(A):** Representative results of time-course analysis of five different sets of experiments. The CD45-negative cell population (%) in PBMNCs and BMCs of the BMP-2-implanted mice was analyzed with flow cytometry for 7 days after BMP-2 implantation. Robust but transient appearance of a CD45-negative population in PBMNCs according to the significant reduction of the CD45-negative population in BMCs within 7 days after BMP-2-implantation was observed in five different sets of experiments compared with nontreated wild-type mice (day 0). **(B):** Analysis of average percentage of CD45-negative population in PBMNCs at peak time within 7 days after BMP-2 implantation in five different sets of experiments showed that the CD45-negative population in PBMNCs was significantly induced by BMP-2-pellet implantation. *, $p = .0000142$. **(C):** Reverse transcription-polymerase chain reaction analysis of the magnetic cell sorting-sorted CD45-negative PBMNCs showed that these cells exhibited Cbfa1 expression before culture (lane 1), additional OP expression in culture without BMP-2 stimulation (lane 2), and ALP and OC expression in culture with BMP-2 stimulation for 3 weeks (300 ng/ml; lane 3). **(D):** The sorted CD45-negative cells cultured in basal medium and in osteogenic medium for 4 weeks showed morphogenic changes to osteoblastic features. Magnification, ×40. Alizarin red staining (right panels) showed that calcium deposition was observed only in cells cultured in osteogenic medium. Magnification, ×40. **(E):** ALP assay showed that ALP activity was increased when the CD45-negative cells in PBMNCs were cultured in osteogenic medium. **(F):** Histologic H&E-stained sections of the hydroxyapatite transplanted in vivo with (right) or without (left) the CD45-negative cells in PBMNCs revealed that those cells could form bone in hydroxyapatite. Magnification, ×100. Abbreviations: ALP, alkaline phosphatase; BMC, bone marrow cell; BMP, bone morphogenetic protein; G3PDH, glyceraldehyde-3-phosphate dehydrogenase; K-A, King-Armstrong; OC, osteocalcin; OP, osteopontin; PBMNC, peripheral blood mononuclear cell.

To determine whether the mobilized CD45-negative cells in the circulation contained MOPCs, we enriched the CD45-negative fraction of the PBMNCs with MACS. The CD45-negative sorted cells already expressed Cbfa1 (Fig. 3C). We cultured the sorted cells in basal medium and examined the expression of osteoblast-specific mRNA in these cells with or without BMP-2 stimulation for 3 weeks. Osteopontin (OP), an early marker of mesenchymal differentiation, started to be expressed in cultures without BMP-2 (Fig. 3C). As expected, the addition of BMP-2 to the culture (300 ng/ml) efficiently induced the expression of osteoblast-specific marker genes such as ALP and OC (Fig. 3C). These results coincided with the data at the protein level that we reported previously [11]. We also observed morphological and functional changes of the CD45-negative sorted cells cultured in the osteogenic medium for 4 weeks. Those cells showed morphologic changes with osteoblastic features, and calcium deposition was clearly observed by alizarin red staining (Fig. 3D). A significant increase in ALP activity was also demonstrated (Fig. 3E). To obtain further evidence of the osteogenic potential of the circulating CD45-negative cells in vivo, we transplanted the fully open interconnected porous calcium hydroxyapatite with or without the cultured circulating CD45-negative cells from GFP-transgenic mice under the muscular fascia in the backs of nude mice (Fig. 3F). Eight weeks later, the hydroxyapatite was harvested and histologically analyzed. Newly formed bone was clearly seen only in the hydroxyapatite with the inoculated CD45-negative cells (Fig. 3F). Immunofluorescence staining showed that the cells in the newly formed bone were GFP-positive, suggesting that not the cells from recipient nude mouse but the transplanted cells with the hydroxyapatite had formed the bone (supplemental online Fig. 2). These data indicate that CD45-negative cells mobilized from bone marrow to the circulating blood contain a major, if not exclusive, population of MOPCs that are derived from bone marrow and provide mature osteoblasts to peripheral tissues.

Characterization of Circulating MOPCs

We further analyzed cell surface markers of the circulating MOPCs in PBMNCs by flow cytometry analysis (Fig. 4). Significant expression of CD44, which is expressed in mesenchymal cells as a receptor of OP [18], was observed (Fig. 4). However, neither hematopoietic lineage markers, such as CD45, CD11b, or Gr-1, nor endothelial lineage markers, such as CD34, Flk-1, or CD31, were detected. Interestingly, circulating CD45-negative MOPCs markedly expressed CXCR4 (Fig. 4), a receptor of the chemokine SDF-1 [19]. The SDF-1 chemokine is known to hold CXCR4-positive stem cells in the bone marrow niche [20–22] and to recruit those cells to peripheral tissues that express SDF-1 [23, 24].

SDF-1 Is Expressed by Vascular Cells and Osteoblasts in and Around the BMP-2 Implant

To determine whether the CXCR4 on the MOPCs played a functional role interacting with SDF-1 for migration to bone formation, we assessed SDF-1 expression in cells surrounding the BMP-2 implant. Immunofluorescence staining showed that CD31-positive and CD34-positive vascular endothelial cells adjacent to the BMP-2 collagen pellet highly expressed SDF-1 (Fig. 5A). The vasculatures expressing SDF-1 are likely to be arterioles, because they express smooth muscle actin at the periphery of the endothelial cells (Fig. 5A). Quantitative real-time PCR analysis also revealed marked elevation of SDF-1 expression in tissues containing BMP-2 pellets from day 1 to day 7 after implantation (Fig.

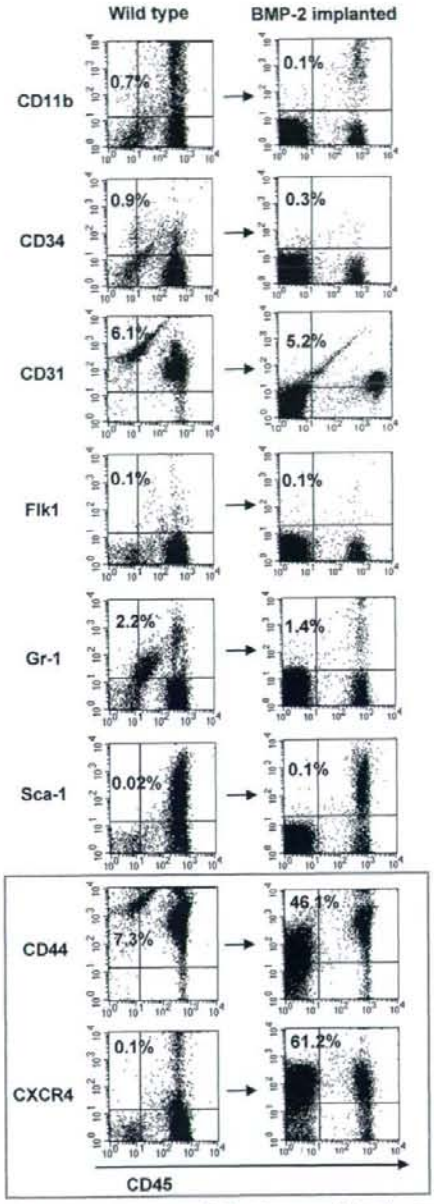

Figure 4. Flow cytometry analysis of marrow-derived osteoblast progenitor cells (MOPCs). Most of the peripheral blood mononuclear cells (PBMNCs) in wild-type mice (control) were CD45-positive. CD45-negative MOPCs were increased in PBMNCs of BMP-2 pellet-implanted mice on day 4. Endothelial lineage markers (CD34, CD31, and Flk1) and hematopoietic lineage markers (CD45, CD11b, and Gr-1) were not detected in the CD45-negative MOPCs in BMP-2-implanted mice. CD44 and CXCR4 were highly expressed in the CD45-negative MOPCs of BMP-2-implanted mice compared with the PBMNCs from wild-type mice. Abbreviation: BMP, bone morphogenetic protein.

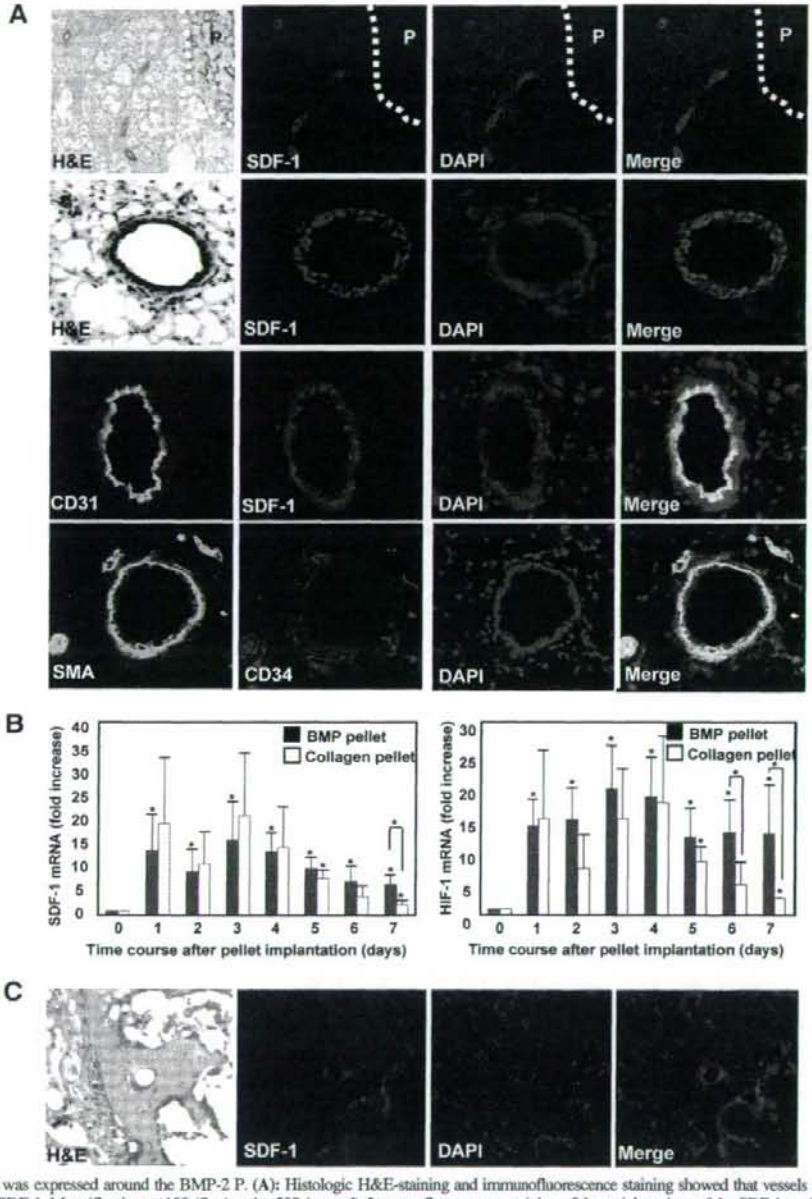

Figure 5. SDF-1 was expressed around the BMP-2 P. **(A):** Histologic H&E-staining and immunofluorescence staining showed that vessels around the BMP-2 P highly expressed SDF-1. Magnification, ×100 (first) and ×500 (second). Immunofluorescence staining of the serial sections of the SDF-1-positive section around the BMP-2 P showed that SDF-1 was expressed from the CD31-, CD34-, and SMA-positive vessel. Magnification, ×500. **(B):** The quantitative time-course analysis of SDF-1 and hypoxia inducible factor-1 (HIF-1) mRNA expression in the BMP-2 and collagen Ps revealed that SDF-1 and HIF-1 expression increased significantly in BMP-2 Ps compared with control tissue (day 0). *, $p < .01$. The high expression was significantly maintained on day 7 in BMP-2 Ps compared with those on day 7 in collagen Ps. *, $p < .01$. The fold increases of expression levels were normalized to those of control tissue (day 0). **(C):** The immunofluorescence staining of the BMP-2-induced ectopic bone on day 14 demonstrated osteoblasts lining the newly formed bone expressed SDF-1. Magnification, ×500. Abbreviations: BMP, bone morphogenetic protein; DAPI, 4′,6-diamidino-2-phenylindole; P, pellet; SDF, stromal cell-derived factor; SMA, smooth muscle actin.

5B). HIF-1, a transcriptional inducer of SDF-1 [23], was also highly elevated in and around the implanted pellets with or without BMP-2 in the early days, suggesting that nonspecific hypoxic conditions in the tissue induced the expression of HIF-1 and SDF-1 (Fig. 5B). After day 6, however, BMP-2 stimulation significantly and specifically sustained the expression of SDF-1 and HIF-1($p < .01$; Fig. 5B), suggesting that the continuous expression of SDF-1 in the regenerating

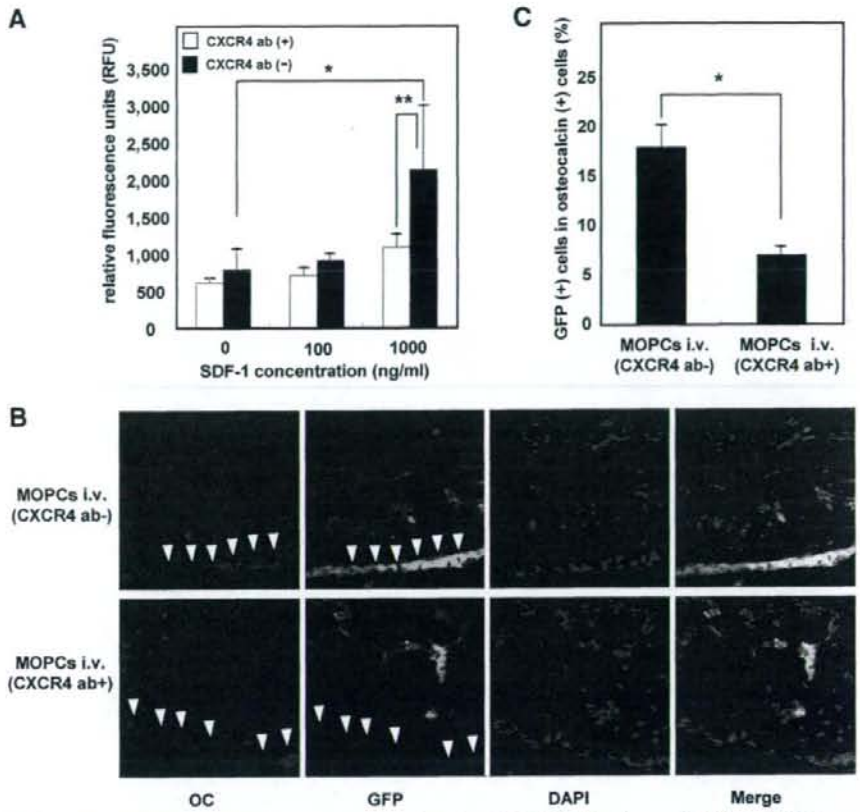

Figure 6. MOPCs in the circulation migrate to the bone formation site in the CXCR4/SDF-1 pathway. **(A):** Effect of SDF-1 on MOPCs in the circulation was checked in the Boyden chamber migration assay. The MOPC migration was stimulated by SDF-1. *, $p < .05$. The effect of SDF-1 was significantly decreased when the MOPCs were pretreated with CXCR4-blocking antibody. **, $p < .05$. The number of migrated cells was measured as RFU. **(B):** MOPCs from a BMP-2-implanted GFP transgenic mice were pretreated with or without the CXCR4-blocking antibody and were injected to a BMP-2-implanted nude mouse daily for 7 days. Immunofluorescence staining of ectopic bone from the nude mouse showed that injected GFP-positive MOPCs differentiated to OC-positive osteoblasts lining the newly formed trabecular bone. Fewer GFP- and OC-positive osteoblasts were found in sections of ectopic bone from a nude mouse injected daily for 7 days with the GFP transgenic MOPCs pretreated with the CXCR4-blocking antibody. Magnification, ×400. **(C):** Quantitative analysis of GFP-positive/OC-positive osteoblasts lining the trabecular bone showed that the MOPC migration was significantly blocked by blocking CXCR4. *, $p = .00019$. Abbreviations: RFU, relative fluorescence units; ab, antibody; DAPI, 4′,6-diamidino-2-phenylindole; GFP, green fluorescent protein; i.v., intravenous; MOPC, marrow-derived osteoblast progenitor cell; OC, osteocalcin; SDF, stromal cell-derived factor.

bone was due to BMP-2 stimulation. This speculation was confirmed by histologic analysis, which clearly indicated sustained SDF-1 expression in the regenerating osteoblasts aligning on the newly formed osseous tissues (Fig. 5C).

The CXCR4/SDF-1 System Plays an Important Role in the Recruitment of Circulating MOPCs to the Region of Ectopic Bone Formation

To examine the chemoattractant potential of SDF-1 for MOPCs in the peripheral blood, MOPCs in PBMNCs isolated from BMP-2 pellet-implanted mice were subjected to in vitro migration assays in a Boyden chamber. Approximately 2.5 times higher migration of the cells was observed in the lower chamber, which contained 1,000 ng/ml SDF-1, and this migration was clearly inhibited by incubating the cells with CXCR4-blocking antibody before the assay ($p < .05$; Fig. 6A). Furthermore, to check the in vivo chemotaxis of circulating MOPCs, we isolated MOPCs from PBMNCs daily from the BMP-2 pellet-implanted GFP-transgenic mice and injected the isolated MOPCs, with or without prior CXCR4-blocking antibody treatment, through the tail veins of BMP-2 pellet-implanted nude mice daily for 7 days. Two weeks later, histologic examination revealed that GFP-positive osteoblasts that originated from injected MOPCs made a significant contribution to ectopic bone formation, and the in vivo migration of the MOPCs to the implanted BMP-2 pellet was strongly inhibited by treatment of the isolated MOPCs with CXCR4-blocking antibody (Fig. 6B; supplemental online Fig. 3). The percentage of GFP-positive osteoblasts in osteocalcin-expressing osteoblasts was significantly decreased to 6.8% ± 0.9% in the ectopic bone by blocking CXCR4 on the MOPCs, whereas the percentage was 17.5% ± 2.3% in the ectopic bone from mice injected with MOPCs without CXCR4 blocking ($p = .00019$; Fig. 6C). These data strongly suggest that CXCR4 on circulating MOPCs functions as a receptor for SDF-1 to induce the migration of MOPCs to the region expressing SDF-1 in regenerating bone.

DISCUSSION

Circulating mesenchymal progenitor cells or osteoblast lineage cells have been shown to exist in various mammals, including humans and mice [6–8, 25, 26]. Those circulating osteoblast lineage cells were isolated from peripheral blood, expanded in culture, and inoculated to show their potency to become osteoblasts in vitro and in vivo. Major questions raised after those observations included where those circulating cells came from, where they went, and how they approached their destination in vivo.

Recently, we reported that marrow cells in intact bone are a major, if not exclusive, source of circulating OPCs under a BMP-2-induced ectopic bone-forming condition in mice, and these cells endogenously participate in the process of the ectopic bone formation [11]. In this study, a parabiotic pairing mouse model showed that ~50% of all osteoblasts were derived from MOPCs in the BMP-2-induced ectopic bone. Previous studies of fracture healing have shown that fracture stimulation induces BMP-2 expression in the surrounding tissues [27–29], suggesting that endogenously circulating MOPCs may also contribute to fracture healing, as well as to ectopic bone formation.

Circulating MOPCs seem to present as a small population without induction. Even after inducing stimulation, the increase of circulating MOPCs was time-limited and not maintained for more than few days. The peak of the MOPC induction in circulation oscillated between day 3 and day 7 after BMP-2 implantation, possibly because of the strength of signals generated by both BMP-2 and injury stimulation (data not shown). These findings may explain the previous difficulties in detecting circulating mesenchymal cells without expansion in culture [30, 31].

SDF-1 has been characterized as a potent CXC chemokine that is constitutively expressed in various cell types, including mesenchymal stem cells and osteoblasts, in bone marrow, and in dermal and synovial fibroblasts [22, 32, 33]. SDF-1 retains hematopoietic stem cells that express CXCR4, a receptor for SDF-1, in bone marrow [21, 22]. SDF-1 expressed in peripheral tissues under inflammatory conditions recruits circulating lymphocytes, monocytes, and other hematopoietic cells, except neutrophils, to the peripheral tissues via the CXCR4/SDF-1 system [34, 35]. A recent study showed that SDF-1 in mural cells around blood vessels functioned to entrap bone marrow-derived vascular endothelial progenitor cells, which express CXCR4, in circulation [36]. We demonstrated significant expression of CXCR4 on circulating MOPCs. A strong expression of SDF-1 was noted not in the circulating MOPCs (supplemental online Fig. 4) but in vascular endothelial cells and osteoblasts in the regions of the ectopic osteogenesis, suggesting that the CXCR4/SDF-1 system may play an important role in entrapping circulating MOPCs around the area of the bone formation, although factors besides SDF-1 may also contribute to the osteogenic processes with MOPCs recruitment. Further analysis showed that elevations of SDF-1 levels were accompanied by upregulation of HIF-1, a well-known transcriptional factor that upregulates SDF-1 expression. HIF-1 and SDF-1 induction were obtained by implantation of the collagen pellet without BMP-2 and probably resulted from the hypoxic tissue damage induced by surgical implantation of the pellet. The BMP-2 pellet, however, exhibited significantly prolonged expression of HIF-1 and SDF-1 at day 7 compared with the collagen pellet itself. This sustained expression of SDF-1 in the BMP-2-pellet was further confirmed in osteoblasts, as well as in vascular endothelial cells of the newly generating bone after day 7 (data not shown). Collectively, HIF-1-dependent initial expression of SDF-1 in arterioles around the BMP-2 pellet seemed to entrap circulating MOPCs, followed by BMP-2-dependent recruitment and differentiation of the trapped MOPCs to osteoblasts, which expressed SDF-1 and may have further enhanced bone formation by continuous recruitment of MOPCs to the osseous tissue in collaboration with the CXCR4/SDF-1 pathway. Previous studies [37, 38] also showed that the CXCR4/SDF-1 pathway plays a pivotal role in the migration of stem cells to regenerating tissues, suggesting that the hypoxic condition induced by tissue injury plays a role in the induction of SDF-1 expression at the initial stage of tissue regeneration.

Recent studies have indicated that CD44 binds to the ubiquitous matrix protein OP and serves as a receptor on CD44-expressing cells to bind to OP [18]. Osteopontin is known to be expressed in osteoblasts and secreted in the areas of the callus formation [39], suggesting that OP functions as the major ligand for CD44 on migrating osteoblast progenitor cells in the remodeling phase of fracture healing [40]. In this context, it is interesting to note that circulating MOPCs significantly expressed CD44 on the cell surface. Interaction between OP and CD44 on MOPCs may be important for the acceleration of bone formation in combination with the CXCR4/SDF-1 system and BMP stimulation.

Signals that trigger migration of the particular cell population from bone marrow to the circulation were not identified in this study. Vascular endothelial growth factor (VEGF) was previously shown to be sufficient for recruitment of marrow-derived vascular endothelial progenitor cells into the circulation [36]. We also observed elevation of VEGF levels in muscular tissue around the implanted collagen pellet (data not shown). This observation may suggest that VEGF contributes to angiogenesis in the area of bone regeneration, although further evidence must be obtained to support this conclusion. Implantation of the collagen pellet itself induced a significant number of MOPCs in the circulation, suggesting that surgical injury may induce production of MOPC-recruiting signals, probably because of hypoxic stress in injured tissue, as previously reported [41]. BMP-2-pellet implantation, however, induced a relatively higher increase in MOPCs in the circulation compared with empty collagen pellets. In addition, subcutaneous injection of BMP-2 without extensive tissue damage could induce ~20% of CD45-negative cells in circulation (data not shown), suggesting that both BMP-2 and tissue injury contribute to the mobilization of MOPCs in circulation. A lack of detectable expression of bone morphogenetic protein receptor II (BMPR-II) on the MOPCs in the circulation (supplemental online Fig. 5) suggests that BMP-2 does not participate in MOPC mobilization but that other factors induced by BMP-2 may. This hypothesis may be supported by our observation that there were no significant changes in the concentration of BMP-2 in serum between wild-type nontreated mice and BMP-2 pellet-implanted mice (supplemental online Fig. 5). Furthermore, we could establish a C57BL/6 mouse bone marrow-derived stromal cell line, which had been shown to be negative for BMPR-II but maintained the capability to differentiate to mature mineralizing osteoblasts when cultured in osteogenic medium (S. Otsuru et al., unpublished data), suggesting that BMPR-II expression may not be essential to maintain osteogenic features in the initial undifferentiated condition of the MOPCs.

The importance of providing additional OPCs to the site of bone formation has been shown by a number of previous studies [42–47]. Identification of signals that induce migration of MOPCs in the circulation may have clinical applications in the future, as the ability to increase MOPCs in the circulation may help patients with intractable bone fractures by inducing further accumulation of MOPCs to the fractured lesion. Robust induction of circulating MOPCs may also enable us to easily isolate these cells by simple blood sampling, providing the possibility

to develop novel cell-based regenerative therapies for intractable bone fractures and possibly for other damaged tissues. Because current procedures to isolate cells directly from bone marrow are invasive, the easy isolation of MOPCs from peripheral blood has advantages in terms of safety, repeatability, and acceptability. Genetic manipulation of isolated MOPCs may also have possible applications in the treatment of genetic disorders such as osteogenesis imperfecta [48, 49].

The potency of circulating MOPCs as stem cells is another issue to be addressed in future studies. Because Sca-1 is an established marker of both mesenchymal and hematopoietic stem cells, MOPCs with low levels of Sca-1 expression seem to have different features compared with stem cells in bone marrow [50, 51]. Demonstration of efficient differentiation activities of MOPCs, in addition to osteoblastic lineage, may illustrate the additional importance of these cells in tissue regeneration.

CONCLUSION

We report here the crucial role of the CXCR4/SDF-1 pathway in the bone formation involving circulating MOPCs. The mobilized MOPCs that expressed CXCR4 were recruited to the bone-forming site by SDF-1 expressed in vascular endothelial cells and the de novo osteoblasts of the region. These data may provide perspective on the use of circulating MOPCs to accelerate bone regeneration in the future.

ACKNOWLEDGMENTS

This work was supported by the Northern Osaka (Saito) Biomedical Knowledge-Based Cluster Creation Project and a Grant-in-Aid from the Ministry of Education, Culture, Sports, Science and Technology of Japan.

DISCLOSURE OF POTENTIAL CONFLICTS OF INTEREST

The authors indicate no potential conflicts of interest.

REFERENCES

1 Jiang Y, Jahagirdar BN, Reinhardt RL et al. Pluripotency of mesenchymal stem cells derived from adult marrow. Nature 2002;418:41–49.
2 Pittenger MF, Mackay AM, Beck SC et al. Multilineage potential of adult human mesenchymal stem cells. Science 1999;284:143–147.
3 Prockop DJ. Marrow stromal cells as stem cells for nonhematopoietic tissues. Science 1997;276:71–74.
4 Minguell JJ, Erices A, Conget P. Mesenchymal stem cells. Exp Biol Med (Maywood) 2001;226:507–520.
5 Pereira RF, Halford KW, O'Hara MD et al. Cultured adherent cells from marrow can serve as long-lasting precursor cells for bone, cartilage, and lung in irradiated mice. Proc Natl Acad Sci U S A 1995;92:4857–4861.
6 Eghbali-Fatourechi GZ, Lamsam J, Fraser D et al. Circulating osteoblast-lineage cells in humans. N Engl J Med 2005;352:1959–1966.
7 Kuznetsov SA, Mankani MH, Gronthos S et al. Circulating skeletal stem cells. J Cell Biol 2001;153:1133–1140.
8 Wan C, He Q, Li G. Allogenic peripheral blood derived mesenchymal stem cells (MSCs) enhance bone regeneration in rabbit ulna critical-sized bone defect model. J Orthop Res 2006;24:610–618.
9 Wozney JM, Rosen V, Celeste AJ et al. Novel regulators of bone formation: Molecular clones and activities. Science 1988;242:1528–1534.
10 Takaoka K, Nakahara H, Yoshikawa H et al. Ectopic bone induction on and in porous hydroxyapatite combined with collagen and bone morphogenetic protein. Clin Orthop Relat Res 1988:250–254.
11 Otsuru S, Tamai K, Yamazaki T et al. Bone marrow-derived osteoblast progenitor cells in circulating blood contribute to ectopic bone formation in mice. Biochem Biophys Res Commun 2007;354:453–458.
12 Okabe M, Ikawa M, Kominami K et al. 'Green mice' as a source of ubiquitous green cells. FEBS Lett 1997;407:313–319.
13 Wright DE, Wagers AJ, Gulati AP et al. Physiological migration of hematopoietic stem and progenitor cells. Science 2001;294:1933–1936.
14 Wakabayashi S, Tsutsumimoto T, Kawasaki S et al. Involvement of phosphodiesterase isozymes in osteoblastic differentiation. J Bone Miner Res 2002;17:249–256.
15 Tamai N, Myoui A, Tomita T et al. Novel hydroxyapatite ceramics with an interconnective porous structure exhibit superior osteoconduction in vivo. J Biomed Mater Res 2002;59:110–117.
16 Nishikawa M, Myoui A, Ohgushi H et al. Bone tissue engineering using novel interconnected porous hydroxyapatite ceramics combined with marrow mesenchymal cells: Quantitative and three-dimensional image analysis. Cell Transplant 2004;13:367–376.
17 Nishikawa M, Ohgushi H, Tamai N et al. The effect of simulated microgravity by three-dimensional clinostat on bone tissue engineering. Cell Transplant 2005;14:829–835.
18 Weber GF, Ashkar S, Glimcher MJ et al. Receptor-ligand interaction between CD44 and osteopontin (Eta-1). Science 1996;271:509–512.
19 Bleul CC, Farzan M, Choe H et al. The lymphocyte chemoattractant SDF-1 is a ligand for LESTR/fusin and blocks HIV-1 entry. Nature 1996;382:829–833.
20 Dar A, Goichberg P, Shinder V et al. Chemokine receptor CXCR4-dependent internalization and resecretion of functional chemokine SDF-1 by bone marrow endothelial and stromal cells. Nat Immunol 2005;6:1038–1046.
21 Ma Q, Jones D, Springer TA. The chemokine receptor CXCR4 is required for the retention of B lineage and granulocytic precursors within the bone marrow microenvironment. Immunity 1999;10:463–471.
22 Nagasawa T, Hirota S, Tachibana K et al. Defects of B-cell lymphopoiesis and bone-marrow myelopoiesis in mice lacking the CXC chemokine PBSF/SDF-1. Nature 1996;382:635–638.
23 Ceradini DJ, Kulkarni AR, Callaghan MJ et al. Progenitor cell trafficking is regulated by hypoxic gradients through HIF-1 induction of SDF-1. Nat Med 2004;10:858–864.
24 Ratajczak MZ, Majka M, Kucia M et al. Expression of functional CXCR4 by muscle satellite cells and secretion of SDF-1 by muscle-derived fibroblasts is associated with the presence of both muscle progenitors in bone marrow and hematopoietic stem/progenitor cells in muscles. STEM CELLS 2003;21:363–371.
25 Fernandez M, Simon V, Herrera G et al. Detection of stromal cells in peripheral blood progenitor cell collections from breast cancer patients. Bone Marrow Transplant 1997;20:265–271.
26 Roufosse CA, Direkze NC, Otto WR et al. Circulating mesenchymal stem cells. Int J Biochem Cell Biol 2004;36:585–597.
27 Bostrom MP. Expression of bone morphogenetic proteins in fracture healing. Clin Orthop Relat Res 1998:S116–S123.
28 Bostrom MP, Lane JM, Berberian WS et al. Immunolocalization and expression of bone morphogenetic proteins 2 and 4 in fracture healing. J Orthop Res 1995;13:357–367.
29 Ishidou Y, Kitajima I, Obama H et al. Enhanced expression of type I receptors for bone morphogenetic proteins during bone formation. J Bone Miner Res 1995;10:1651–1659.
30 Lazarus HM, Haynesworth SE, Gerson SL et al. Human bone marrow-derived mesenchymal (stromal) progenitor cells (MPCs) cannot be recovered from peripheral blood progenitor cell collections. J Hematother 1997;6:447–455.
31 Wexler SA, Donaldson C, Denning-Kendall P et al. Adult bone marrow is a rich source of human mesenchymal 'stem' cells but umbilical cord and mobilized adult blood are not. Br J Haematol 2003;121:368–374.
32 Nagasawa T, Nakajima T, Tachibana K et al. Molecular cloning and characterization of a murine pre-B-cell growth-stimulating factor/stromal cell-derived factor 1 receptor, a murine homolog of the human immunodeficiency virus 1 entry coreceptor fusin. Proc Natl Acad Sci U S A 1996;93:14726–14729.
33 Zvaifler NJ, Marinova-Mutafchieva L, Adams G et al. Mesenchymal precursor cells in the blood of normal individuals. Arthritis Res 2000;2:477–488.
34 Aiuti A, Webb IJ, Bleul C et al. The chemokine SDF-1 is a chemoattractant for human CD34+ hematopoietic progenitor cells and provides a new mechanism to explain the mobilization of CD34+ progenitors to peripheral blood. J Exp Med 1997;185:111–120.

35 Bleul CC, Fuhlbrigge RC, Casasnovas JM et al. A highly efficacious lymphocyte chemoattractant, stromal cell-derived factor 1 (SDF-1). J Exp Med 1996;184:1101–1109.
36 Grunewald M, Avraham I, Dor Y et al. VEGF-induced adult neovascularization: Recruitment, retention, and role of accessory cells. Cell 2006; 124:175–189.
37 Imitola J, Raddassi K, Park KI et al. Directed migration of neural stem cells to sites of CNS injury by the stromal cell-derived factor 1alpha/CXC chemokine receptor 4 pathway. Proc Natl Acad Sci U S A 2004; 101:18117–18122.
38 Ji JF, He BP, Dheen ST et al. Interactions of chemokines and chemokine receptors mediate the migration of mesenchymal stem cells to the impaired site in the brain after hypoglossal nerve injury. STEM CELLS 2004;22:415–427.
39 Hirakawa K, Hirota S, Ikeda T et al. Localization of the mRNA for bone matrix proteins during fracture healing as determined by in situ hybridization. J Bone Miner Res 1994;9:1551–1557.
40 Yamazaki M, Nakajima F, Ogasawara A et al. Spatial and temporal distribution of CD44 and osteopontin in fracture callus. J Bone Joint Surg Br 1999;81:508–515.
41 Rochefort GY, Delorme B, Lopez A et al. Multipotential mesenchymal stem cells are mobilized into peripheral blood by hypoxia. STEM CELLS 2006;24:2202–2208.
42 Curylo LJ, Johnstone B, Petersilge CA et al. Augmentation of spinal arthrodesis with autologous bone marrow in a rabbit posterolateral spine fusion model. Spine 1999;24:434–438; discussion 438–439.
43 Grundel RE, Chapman MW, Yee T et al. Autogeneic bone marrow and porous biphasic calcium phosphate ceramic for segmental bone defects in the canine ulna. Clin Orthop Relat Res 1991:244–258.
44 Lindholm TS, Nilsson OS, Lindholm TC. Extraskeletal and intraskeletal new bone formation induced by demineralized bone matrix combined with bone marrow cells. Clin Orthop Relat Res 1982:251–255.
45 Lindholm TS, Ragni P, Lindholm TC. Response of bone marrow stroma cells to demineralized cortical bone matrix in experimental spinal fusion in rabbits. Clin Orthop Relat Res 1988:296–302.
46 Takagi K, Urist MR. The role of bone marrow in bone morphogenetic protein-induced repair of femoral massive diaphyseal defects. Clin Orthop Relat Res 1982:224–231.
47 Werntz JR, Lane JM, Burstein AH et al. Qualitative and quantitative analysis of orthotopic bone regeneration by marrow. J Orthop Res 1996;14:85–93.
48 Chamberlain JR, Schwarze U, Wang PR et al. Gene targeting in stem cells from individuals with osteogenesis imperfecta. Science 2004;303: 1198–1201.
49 Horwitz EM, Prockop DJ, Fitzpatrick LA et al. Transplantability and therapeutic effects of bone marrow-derived mesenchymal cells in children with osteogenesis imperfecta. Nat Med 1999;5:309–313.
50 Meirelles LS, Nardi NB. Murine marrow-derived mesenchymal stem cell: Isolation, in vitro expression, and characterization. Br J Haematol 2003;123:702–711.
51 Baddoo M, Hill K, Wilkinson R et al. Characterization of mesenchymal stem cells isolated from murine bone marrow by negative selection. J Cell Biochem 2003;89:1235–1249.

See www.StemCells.com for supplemental material available online.

Oncogene (2008) 27, 1821–1833
© 2008 Nature Publishing Group All rights reserved 0950-9232/08 $30.00
www.nature.com/onc

ORIGINAL ARTICLE

Cold shock domain protein A represses angiogenesis and lymphangiogenesis via inhibition of serum response element

Y Saito[1,2], H Nakagami[1], M Kurooka[1], Y Takami[1], Y Kikuchi[1], H Hayashi[1], T Nishikawa[1], K Tamai[1], R Morishita[3], N Azuma[2], T Sasajima[2] and Y Kaneda[1]

[1]*Division of Gene Therapy Science, Graduate School of Medicine, Osaka University, Osaka, Japan;* [2]*Department of Surgery, Asahikawa Medical University, Hokkaido, Japan and* [3]*Division of Clinical Gene Therapy, Graduate School of Medicine, Osaka University, Osaka, Japan*

Dual-targeted therapy for antiangiogenesis and antilymphangiogenesis represents a potentially effective strategy for the treatment of various malignancies. Therefore, the goal of the present study was to identify genes that encode inhibitors of both angiogenesis and lymphangiogenesis. Using a cDNA library obtained from Lewis lung carcinoma (LL/2), a candidate gene was identified by the evaluation of growth inhibition in aortic and lymphatic endothelial cells (EC) as that coding for the mouse cold shock domain protein A (mCSDA). Overexpression of mCSDA significantly repressed cell proliferation and c-*fos* promoter activity in aortic, venous and lymphatic ECs. CSDA is a DNA-binding protein that binds to the hypoxia response element (HRE). Furthermore, of importance, we revealed that CSDA could directly bind to the serum response element (SRE) sequence, resulting in the inhibition of SRE activity, which may lead to growth inhibition in ECs. In an LL/2-inoculated mouse model, tumor growth was significantly repressed in an mCSDA-injected group. Histopathological analysis revealed that expression of blood and lymphatic EC markers was significantly decreased in mCSDA-injected groups. In conclusion, these data suggest that expression of CSDA can repress angiogenesis and lymphangiogenesis via direct binding to SRE in addition to HRE.

Oncogene (2008) **27,** 1821–1833; doi:10.1038/sj.onc.1210824; published online 15 October 2007

Keywords: antiangiogenesis; antilymphangiogenesis; gene therapy; endothelial cell serum response element

Introduction

Normal tissue growth, repair and regeneration require ingrowth of blood vessels (angiogenesis) and lymphatics (lymphangiogenesis) to provide proper nutrition and drainage, respectively. However, a similar process governs the uncontrolled growth and spread of various malignancies (Sleeman, 2000; Pepper, 2001). Indeed, the capacity of tumor cells to induce angiogenesis and lymphangiogenesis may determine the probability of vascular or lymphatic spread of malignancy.

The concept of antiangiogenic therapy was first proposed in the early 1970s as a method of restricting tumor growth (Folkman, 1971). Many different strategies for antiangiogenesis have been investigated, including those that target endothelial cells (EC) (that is, the anti-vascular endothelial growth factor (VEGF) antibody) (Kim *et al.*, 1993), mural and stromal cells (Bergers *et al.*, 2003), hematopoietic cells (Kaplan *et al.*, 2005; Zou, 2005) or neoplastic cells (Izumi *et al.*, 2002). Furthermore, angiogenesis inhibitors are currently in clinical use worldwide for the treatment of various cancers (Folkman, 2006).

More recently, several studies have reported an association between VEGF-C expression, tumor lymphangiogenesis and lymph node metastasis in many cancers, including thyroid (Bunone *et al.*, 1999), prostate (Tsurusaki *et al.*, 1999), gastric (Yonemura *et al.*, 1999), colorectal (Akagi *et al.*, 2000) and lung cancers (Niki *et al.*, 2000). For example, investigators have reported that overexpression of VEGF-C or -D induces lymphangiogenesis and promotes tumor metastasis in mouse tumor models (Karpanen *et al.*, 2001; Mandriota *et al.*, 2001; Skobe *et al.*, 2001; Stacker *et al.*, 2001), which suggests that lymphatic vessels also regulate tumor metastasis. Indeed, a soluble VEGF receptor (VEGFR)-3-immunoglobulin (Ig) fusion protein has been shown to inhibit VEGF-C-induced tumor lymphangiogenesis (Karpanen *et al.*, 2001).

In combination, these data suggest that simultaneous targeting of angiogenesis and lymphangiogenesis is an ideal strategy for the treatment of various malignancies in views of antitumor growth and antimetastasis. Therefore, the goal of the present study was to identify novel therapeutic genes that repress both angiogenesis and lymphangiogenesis.

Results

Screening for candidate antiangiogenesis/antilymphangiogenesis genes

A cDNA library obtained from Lewis lung carcinoma (LL/2) was used to screen for candidate genes based on the

Correspondence: Prof. Y Kaneda, Division of Gene Therapy Science, Graduate School of Medicine, Osaka University, 2-2 Yamadaoka, Suita, Osaka 565-0871, Japan.
E-mail: kaneday@gts.med.osaka-u.ac.jp
Received 31 January 2007; revised 24 July 2007; accepted 30 August 2007; published online 15 October 2007

Folkman's hypothesis applied at discovery of angiostatin and endostatin that cancer cells might produce factors related to not only promoters of angiogenesis and lymphangiogenesis, but also inhibitors of them (Folkman, 2006). The first screening was performed in canine lymphatic endothelial cells (cLEC) by modified 3-(4,5-dimethylthiazol-2-yl)-2,5-diphenyltetrazolium bromide (MTS) assay using the indirect functional screening method with the hemagglutinating virus of Japan envelope (HVJ-E) vector, as previously reported (Nishikawa *et al.*, 2006). Canine LEC is much superior to human LEC (hLEC) about transfection efficiency and sensitivity of MTS assay (data not shown), as same as relationship of bovine aortic endothelial cells (BAEC) and human AEC (HAEC). This process resulted in identification of 22 candidate antilymphangiogenic genes from the well number 88, which had the lowest value of the cLEC proliferation (Figure 1a). Further screening was performed on BAEC by the direct evaluation of c-*fos* promoter activity after co-transfection with each candidate gene (Figure 1b). Gene number 6 had the lowest value in terms of c-*fos* promoter activity. Gene sequencing revealed that this plasmid DNA sequence matched that encoding the mouse cold shock domain protein A (mCSDA) cDNA (GenBank accession number NM139117.2), which is localized to chromosome 6. Although the reported full open reading frame length of mCSDA was 1086 bp, the plasmid reading frame length was 888 bp because it lacked part of exon 1 (from 67 to 175 bp of the open reading frame). Repeat subcloning of mCSDA from the LL/2 cDNA library by PCR yielded similar results in terms of deletion profiles. Therefore, subsequent experiments utilized this deletion-modified mCSDA sequence.

Expression of mCSDA

Immunofluorescent staining demonstrated that overexpressed mCSDA tagged with hemagglutinin (HA) was localized to the nucleus until at least 48 h after transfection (Figure 2a). Furthermore, northern blotting demonstrated CSDA mRNA expression in the heart and skeletal muscle of several human tissues, as previously reported (Figure 2b) (Kudo *et al.*, 1995). In whole murine embryos, CSDA mRNA was present in low levels until embryonic day 15, and was highly detected at embryonic day 17 (Figure 2b). Endogenous expression of CSDA was detected in several types of ECs by reverse transcription–PCR (RT–PCR) (Figure 2c). Interestingly, mCSDA was expressed in aortic and venous ECs and, to a lesser extent, in lymphatic EC, but was barely detected in human aortic smooth muscle cell (HASMC) ($P<0.001$; Figure 2d).

Function of mCSDA on LL/2 and ECs

Endogenous expression of CSDA was detected in LL/2 by RT–PCR (Figure 3a). Furthermore, mCSDA mRNA level was upregulated by overexpression of mCSDA plasmid, and was knocked down by RNA interference (RNAi) using small interfering RNA (siRNA). In fact, transfection of siRNA resulted in a 93% decrease in mCSDA mRNA levels, as quantified by real-time RT–PCR. To investigate whether mCSDA has an effect on LL/2 proliferation, mCSDA plasmid or siRNA for mCSDA was transferred into LL/2. Overexpression or repression of mCSDA expression in the cells resulted in no significant change in cellular proliferation, as assessed by MTS assay and *c-fos* promoter activity after co-transfection with the c-*fos*-luciferase reporter gene (Figure 3b).

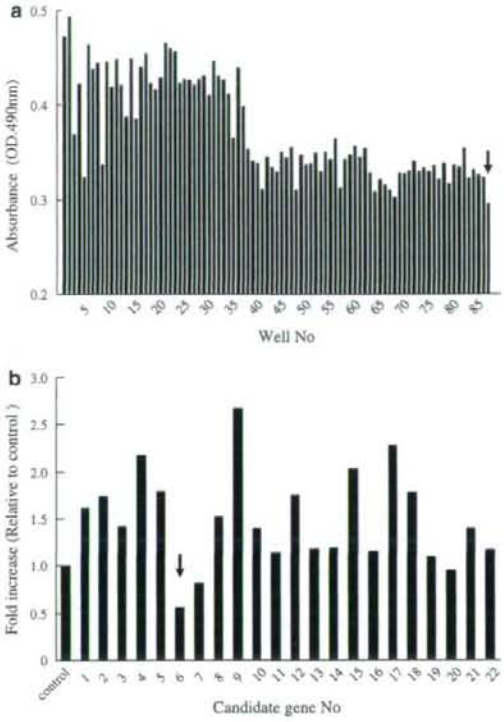

Figure 1 Screening for antiangiogenesis and antilymphangiogenesis gene. (**a**) The first screening was performed using the indirect functional screening method with the HVJ-E vector. Well no. 88 has the lowest cLEC proliferation value as determined by MTS assay (arrow). (**b**) Effect of 22 candidate genes on c-*fos* promoter activity in BAEC. GFP plasmid was transfected as control. The c-*fos* promoter activity of no. 6 was the lowest (arrow).

Next, to confirm the inhibitory effect of mCSDA on EC growth, vascular or lymphatic ECs were co-transfected with the c-*fos*-luciferase reporter gene and mCSDA plasmid. Overexpression of mCSDA significantly repressed c-*fos* promoter activity in HAEC, human umbilical vein endothelial cell (HUVEC), hLEC and cLEC, when compared with cells transfected with control plasmid ($P<0.001$; Figure 3c). These results demonstrated that mCSDA had inhibitory effect directly on the proliferation of vascular and lymphatic ECs.

Functional domain analysis of mCSDA

The effect of the deletion-modified mCSDA was compared with that of the full human CSDA (hCSDA)

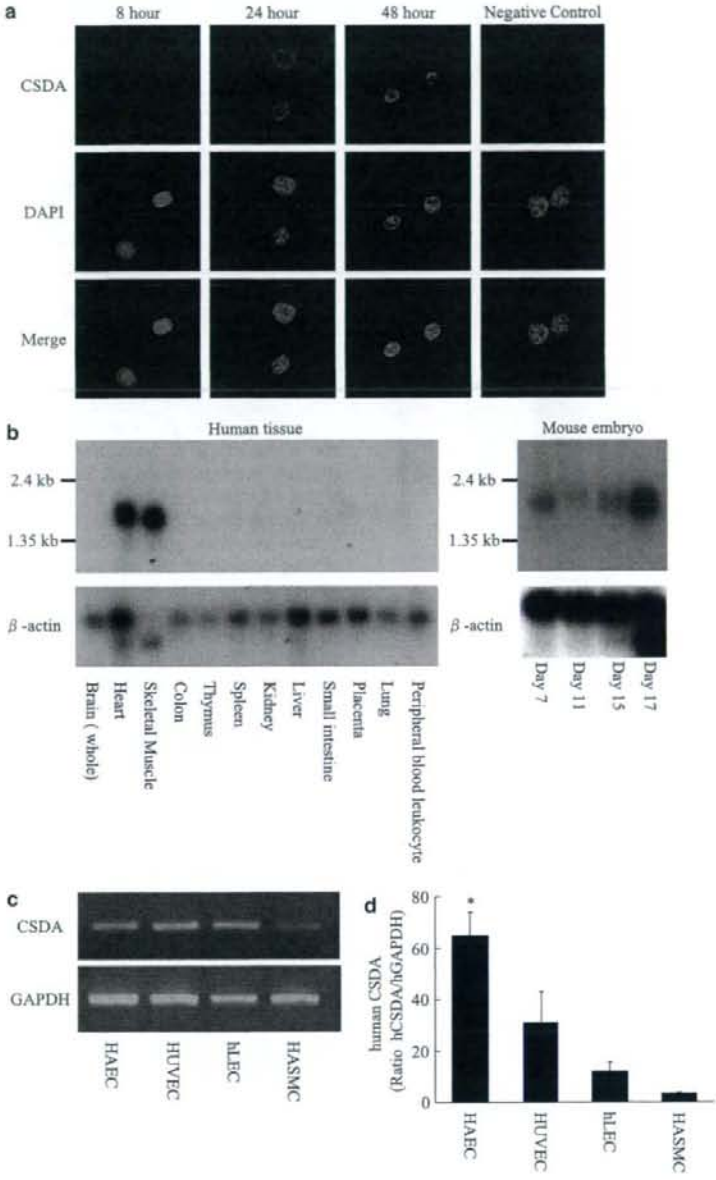

Figure 2 Cold shock domain protein A (CSDA) expression. (**a**) Representative pictures of immunofluorescent stains in COS7 at three time points. 'CSDA' indicates staining with anti-HA antibody (red), 'DAPI' indicates nuclear staining (blue), and 'Merge' indicates staining with both (× 400 magnification). (**b**) Expression patterns of CSDA in several human tissues as demonstrated by northern blotting. Corresponding β-actin expression was used to standardize loading (left panels). Timing of expression in the developing mouse embryo by northern blot. Corresponding β-actin expression was used to standardize loading (right panels). (**c** and **d**) Expression of endogenous human CSDA by RT–PCR (**c**) and quantitative real-time RT–PCR (**d**) in human aortic endothelial cells (HAEC), human umbilical vein endothelial cell (HUVEC), human lymphatic endothelial cells (hLEC) and HASMC. $^{*}P<0.001$ vs human aortic smooth muscle cell (HASMC).

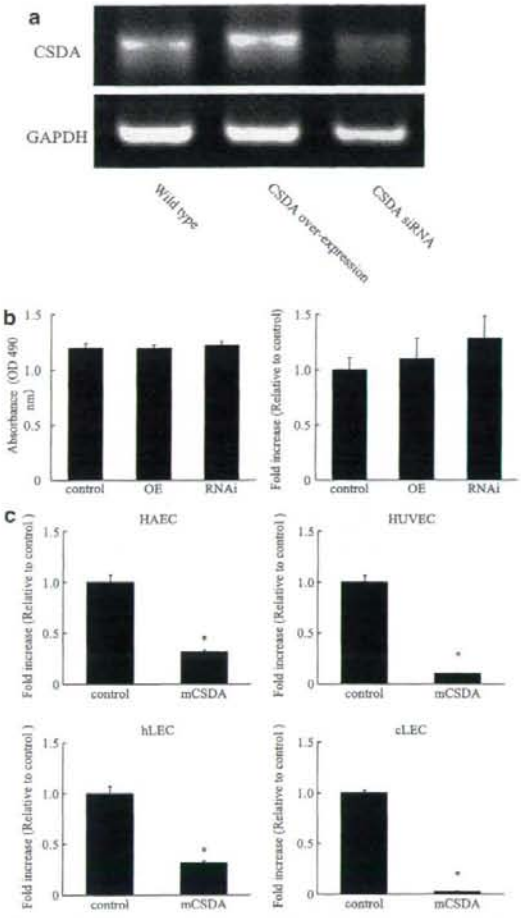

Figure 3 Function of mouse cold shock domain protein A (mCSDA) in LL/2 and ECs. (**a**) Expression of mCSDA transcript in LL/2, wild-type (left), mCSDA overexpression (OE; middle) and RNA interference (RNAi) for mCSDA (right). (**b**) Effect of overexpressed mCSDA plasmid or RNAi for mCSDA on LL2 proliferation, as determined by MTS assay (left panel) and c-*fos* promoter assay (right panel). GFP plasmid was transfected as control. $n=6$. (**c**) Effect of overexpressed mCSDA plasmid on c-*fos* promoter activity in human aortic endothelial cells (HAEC), human umbilical vein endothelial cell (HUVEC), hLEC and canine lymphatic endothelial cells (cLEC). GFP plasmid was transfected as control ($n=6$, $^*P<0.001$ vs control).

sequence using a c-*fos* promoter assay in BAEC or cLEC. Overexpressed mCSDA and hCSDA showed a similar inhibitory effect on c-*fos* promoter activity in both EC types ($P<0.001$; Figure 4a). Since hCSDA could directly bind the promoter region of DNA via exon 1–5, leading to suppression of transcription (Kudo *et al.*, 1995), the importance of exon 1–5 containing cold shock domain (CSD) in mCSDA was investigated by construction of deletion mutants (DMs). As shown in Figure 4b, three types of DM mCSDA were constructed. DM1 possessed the CSD, whereas DM2 and DM3 lacked the CSD. DM3 also lacked the nuclear localization signal. The c-*fos* promoter activity was significantly decreased in both of the ECs that overexpressed DM1, but not in ECs that overexpressed DM2 and DM3 without the CSD ($P<0.001$; Figure 4c). These results suggest that the CSD plays a key role in the inhibition of EC proliferation.

Mechanisms of mCSDA in ECs

We next focused on the mechanism of EC-proliferated inhibition by mCSDA. Although CSDA inhibits VEGF-A promoter activity by competitive binding with hypoxia inducible factor-1 (HIF-1) to the hypoxia response element (HRE) (Coles *et al.*, 2002), the key factor of lymphatic EC proliferation is not VEGF-A, but VEGF-C. Furthermore, there is no HIF-1 binding site in the VEGF-C promoter (Chilov *et al.*, 1997). Thus, the new mechanism of mCSDA was required to explain about repression of both EC types in our results. Since we hypothesized that mCSDA have a potential to widely inhibit effect of growth factors, such as VEGF-A and -C, we compared the cell proliferations with or without the treatment of fetal bovine serum (FBS) as a common paracrine factor on ECs. Indeed, transfection of ECs with mCSDA resulted in a decrease in serum-induced cellular proliferation, as demonstrated by MTS assay ($P<0.05$; Figure 5a). Furthermore, cells co-transfected with the c-*fos*-luciferase reporter gene and mCSDA plasmid showed decreased serum-induced c-*fos* promoter activity when compared with those transfected with control plasmid ($P<0.05$; Figure 5b).

The ras/extracellular signal-regulated kinase (ERK) pathway provides a common route of signals from different growth factor receptors, and is a key signaling pathway for the regulation of aortic and lymphatic EC proliferation (Figure 5c) (Nakagami *et al.*, 2001; Saito *et al.*, 2006). Consistent with previous reports, ERK was phosphorylated by treatment with recombinant hepatocyte growth factor (HGF) in ECs. However, overexpression of mCSDA did not inhibit the phosphorylation of ERK in BAEC (Figure 5d). Because mCSDA was reported as a repressor of a number of growth factors (Shannon *et al.*, 2001), experiments were conducted to determine whether mCSDA could repress the serum response element (SRE), which is the binding site of the last signal of the ERK pathway and also exists in the c-*fos* promoter.

SRE activity was further evaluated by co-transfection with the SRE-luciferase reporter gene and mCSDA plasmid. Overexpressed CSDA significantly decreased SRE activity compared with that of control plasmid in HAEC, HUVEC, hLEC and cLEC ($P<0.05$; Figure 6a). These data suggest that mCSDA could inhibit the SRE activation without inhibition of ERK activation. Similarly, ECs co-transfected with the SRE-luciferase reporter gene and mCSDA plasmid showed decreased serum-induced SRE activity when compared with that of cells transfected with control plasmid ($P<0.05$; Figure 6b).

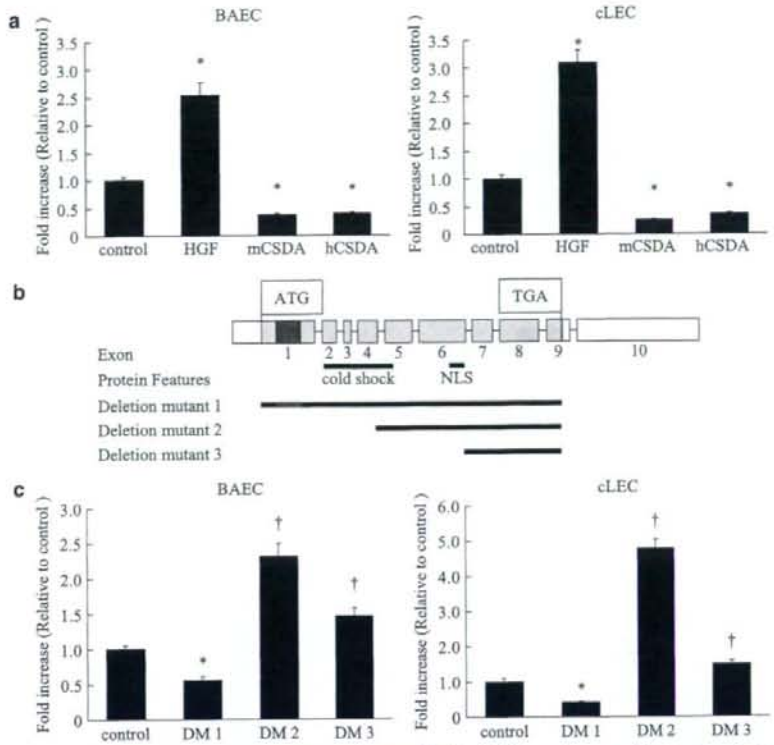

Figure 4 Domain analysis of mouse cold shock domain protein A (mCSDA). (**a**) Effect of mouse mCSDA plasmid, which lacked part of exon 1, and human CSDA (hCSDA) plasmid on c-*fos* promoter activity in bovine aortic endothelial cells (BAEC) and canine lymphatic endothelial cells (cLEC). GFP plasmid was transfected as control, and hepatocyte growth factor (HGF) plasmid was transfected as a positive control ($n=6$, $^*P<0.001$ vs control). (**b**) Schema of constructs for deletion mutants of mCSDA. mCSDA plasmid lacked a part of exon 1 (red bar). Deletion mutant 1 (DM1); from exon 1 to 9 without part of exon 1 (red line), deletion mutant 2 (DM2); from exon 4 to 9 without CSD, deletion mutant 3 (DM3); from exon 6 to 9 without CSD and the nuclear localization signal (NLS). (**c**) Comparison of deletion mutants of mCSDA on c-*fos* promoter activity in BAEC and cLEC. GFP plasmid was transfected as control ($n=6$, $^*P<0.001$ vs control, $^\dagger P<0.001$ vs DM 1).

Because CSD proteins could repress via direct binding to CT-rich DNA sequence (Shannon *et al*., 1997), we hypothesized that mCSDA could directly bind to the SRE sequence to repress the cell growth. Gel mobility shift assay demonstrated that overexpression of the mCSDA gene increased specific binding to the consensus SRE sequence but not to any mutant SRE sequence. Furthermore, preincubation of nuclear extract with anti-CSDA antibody blocked formation of mCSDA–SRE complex. These results indicate that mCSDA could directly bind to the SRE sequence (Figure 6c).

Antiangiogenesis and antilymphangiogenesis in vivo

Given the *in vitro* data, we hypothesized that mCSDA would repress tumor angiogenesis and lymphangiogenesis using an LL/2-inoculated mouse model, which was known as a model of the angiogenesis-dependent tumor growth (Supplementary Figure S1a) (Watanabe *et al*., 2004), and in Figure 3, we have already confirmed that mCSDA did not directly influence with LL/2 growth. In an LL/2-inoculated mouse model, transfer of mCSDA into the boundary area between tumor and normal tissue was performed using the ultrasound-sonoporation method (Supplementary Figure S1b) (Shimamura *et al*., 2004), and tumor size was measured over the subsequent 21 days.

On the flank model at day 21 after LL/2 inoculation, many mature feeding arteries were connected from the host normal tissue to tumor on the green fluorescent protein (GFP)-injected group (control group), but a few weak arteries on mCSDA-injected group (CSDA group) (Figure 7a). The blood flow by laser Doppler image was significantly lower around the tumor in the CSDA group compared with that in the control group ($P<0.01$; Figure 7a). Correspondingly, tumor volume ($P<0.01$) and weight ($P<0.05$) was significantly lower in the CSDA group when compared with the control group (Figure 7b). Furthermore, in this flank model at 21 days after LL/2 inoculation tumor had spread to the

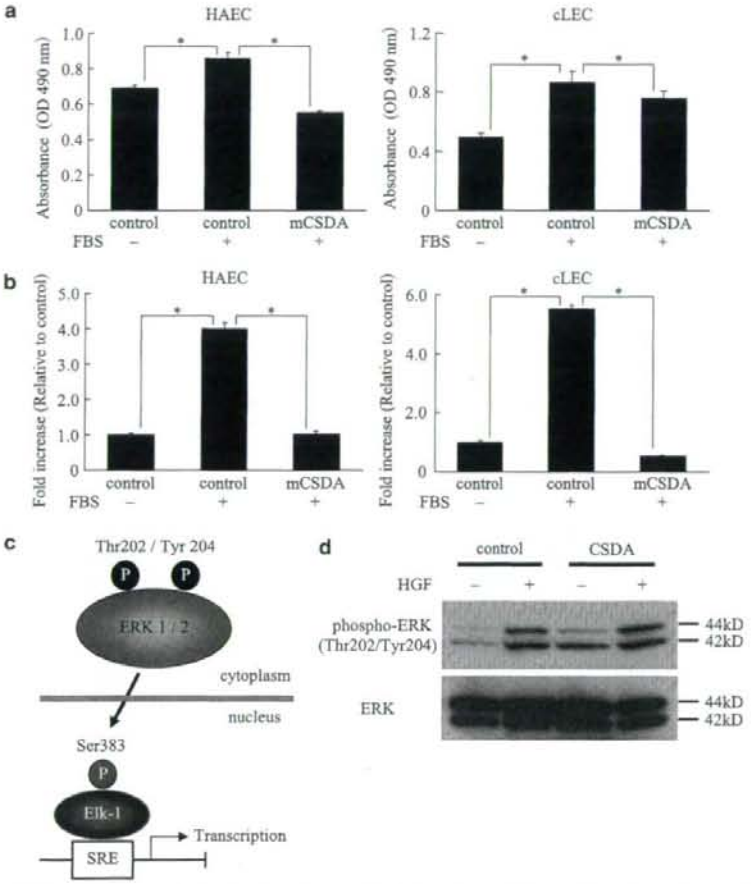

Figure 5 Mechanism of mouse cold shock domain protein A (mCSDA) function in ECs. (**a**) Effect of mCSDA plasmid with or without fetal bovine serum (FBS) on human aortic endothelial cells (HAEC) and canine lymphatic endothelial cells (cLEC), as demonstrated by the MTS assay. ECs were transfected with mCSDA plasmid or GFP plasmid as control, and cultured in FBS-free medium (FBS −) or 10% FBS medium (FBS +). (**b**) Effect of mCSDA plasmid with or without FBS on HAEC and cLEC, as demonstrated by the c-*fos* promoter assay. ECs were transfected with mCSDA plasmid or GFP plasmid as control and then cultured in FBS-free medium (FBS −) or 10% FBS medium (FBS +) ($n=8$, $^*P<0.05$). (**c**) Schematic diagram of the signaling pathways of ERK. (**d**) Typical western blot of total ERK and phosphorylated ERK in BAEC transfected with mCSDA plasmid or GFP plasmid as control, before, and 10 min after treatment with human recombinant hepatocyte growth factor (HGF, 10 ng ml^{-1}).

lung in the control group, and the number of lung metastasis in the CSDA group was significantly decreased compared with control group ($P<0.001$; Figures 7c and d). The metastasis in lung and inguinal lymph node was also diagnosed by hematoxylin and eosin (H&E) stain (Figure 7e). We further focused on the histopathological analysis of the boundary area (connecting tissue area) between the main tumor and normal tissue by immunofluorescent staining. Of importance, expression of EC marker, von Willebrand factor (vWF), was low in the normal tissue but high in the tumor tissue in the CSDA group (Figure 8a). At the boundary area between tumor and normal tissue, the expression of EC markers (vWF and PECAM-1) and capillary density was significantly decreased in CSDA group when compared with the control group ($P<0.01$; Figures 8b and c). Furthermore, expression of lymphatic EC marker (Prox1) was only seen in tumor tissue (Figure 9a), and on the magnification images the expression of lymphatic EC markers (Prox1 and LYVE-1) was decreased in the CSDA groups (Figure 9b). Indeed, the number of lymphatic vessels was significantly decreased in the CSDA group compared with control group ($P<0.05$; Figure 9c).

To further evaluate the metastasis of LL/2 inoculation, we created footpad model, which initially spreads to the inguinal lymph node, using LL/2 stable transfectant expressing luciferase. We also injected the patent blue-staining